SCIENTIFIC REPORTS
nature research

OPEN

Simulated CO_2-induced ocean acidification for ocean in the East China: historical conditions since preindustrial time and future scenarios

Han Zhang[1,2] & Kuo Wang[1*]

Since preindustrial times, as atmospheric CO_2 concentration increases, the ocean continuously absorbs anthropogenic CO_2, reducing seawater pH and $[CO_3^{2-}]$, which is termed ocean acidification. We perform Earth system model simulations to assess CO_2-induced acidification for ocean in the East China, one of the most vulnerable areas to ocean acidification. By year 2017, ocean surface pH in the East China drops from the preindustrial level of 8.20 to 8.06, corresponding to a 35% rise in $[H^+]$, and reduction rate of pH becomes faster in the last two decades. Changes in surface seawater acidity largely result from CO_2-induced changes in surface dissolved inorganic carbon (DIC), alkalinity (ALK), salinity and temperature, among which DIC plays the most important role. By year 2300, simulated reduction in sea surface $[CO_3^{2-}]$ is 13% under RCP2.6, contrasted to 72% under RCP8.5. Furthermore, simulated results show that CO_2-induced warming acts to mitigate reductions in $[CO_3^{2-}]$, but the individual effect of oceanic CO_2 uptake is much greater than the effect of CO_2-induced warming on ocean acidification. Our study quantifies ocean acidification induced by anthropogenic CO_2, and indicates the potentially important role of accelerated CO_2 emissions in projections of future changes in biogeochemistry and ecosystem of ocean in the East China.

Atmospheric CO_2 concentration has reached 407.44 ± 0.10 ppm (parts per million) by year 2018, increased by 46% since preindustrial time[1], which is mainly due to human activities of fossil fuel burning and land use changes. Observational-based estimates show that, during year 1750 and 2017, total anthropogenic CO_2 emission is 660 ± 95 PgC (1 PgC $= 10^{15}$ grams of carbon $=$ 1 billion tons of carbon)[2]. About 42% of these emissions stayed in the atmosphere, meanwhile, about 25% and 33% of the emissions were absorbed by the ocean and terrestrial biosphere, respectively[2].

The rise of atmospheric CO_2 concentration results in global warming through trapping long wave radiation, a process known as greenhouse effect[3–6]. Global warming could alter physical, chemical, and biological processes in the ocean[7–10]. Oceanic uptake of CO_2 could buffer part of the global warming; however, not only global warming, the penetration of anthropogenic CO_2 would also perturb ocean chemistry by making seawater more acidic, which is termed as ocean acidification[11].

Generally, ocean acidification is caused primarily by oceanic CO_2 uptake from the atmosphere. In addition, especially in the coastal seas, there are some other factors that could also lead to the acidification of seawater. For example, increasing input of anthropogenic nitrogen to the ocean, and the resultant changes in organic matter production, oxidation, and deoxygenation, may have effects on ocean acidification[12]. However, many recent studies suggested that impacts of biological nitrogen assimilation and release on ocean acidification are negligible compared with impacts of CO_2 absorption[13,14]. Variations in riverine carbon fluxes to the ocean could either accelerate or offset seawater acidity in coastal areas, revealing large uncertainties[15]. Also, some processes in the ocean $CaCO_3$ cycle, including calcification and ballast effects, could also trigger feedbacks to ocean acidification[16–18]. This study will focus on the individual effect of oceanic CO_2 uptake on ocean acidification, which is

[1]Zhejiang Climate Center, Hangzhou, Zhejiang, 310017, China. [2]Department of Atmospheric Sciences, School of Earth Sciences, Zhejiang University, Hangzhou, Zhejiang, 310027, China. *email: wangkuo.climate@qq.com

generally considered a key process affecting seawater acidity and the ocean carbon cycle in the East China. In addition, we also assess the effect of CO_2-induced warming on ocean acidification, and compare the strength of individual effects of oceanic CO_2 uptake and CO_2-induced warming on ocean acidification in the East China.

Seawater pH is known as a measurement to quantify the degree of ocean acidification. Since the industrial revolution, sea surface pH ($pH = -\log_{10}[H^+]$) has dropped by about 0.1 units by year 2013, corresponding to an increase of 26% in hydrogen ion concentration ($[H^+]$)[19]. The current pH reduction rate is likely to be the highest during the past hundreds of thousands of years[20]. The elevated hydrogen ion concentration tended to reduce carbonate ion concentration ($[CO_3^{2-}]$) via:

$$H^+ + CO_3^{2-} \rightarrow HCO_3^- \quad (1)$$

The reduction in carbonate ion concentration would lower seawater calcium carbonate ($CaCO_3$) saturation state (Ω) for aragonite or calcite (two different polymorphs of $CaCO_3$), which is defined as:

$$\Omega = [Ca^{2+}][CO_3^{2-}]/K_{sp}^* \quad (2)$$

where K_{sp}^* is the stoichiometric solubility product constant with respect to aragonite or calcite[3,21].

The main concern of ocean acidification originates from the potentially adverse impacts of $CaCO_3$ saturation state reductions on marine calcifying organisms, which use $CaCO_3$ to form their skeletons or shells. For instance, reduced Ω could decrease calcification rate of calcifying organisms[22–28], and increase $CaCO_3$ dissolution rate[29–34], making their skeletons or shells vulnerable. In addition, by conducting meta-analyses of case studies, Jin *et al.* (2015) suggested, during the past decade, the echinoderm/microbenthic productivity has been altered in the seas around China, which has implications for the effects of ocean acidification on marine ecosystem[35]. Concluded from laboratory experiments, Liu and He (2012) also provided evidences of the potentially important impacts of ocean acidification on metabolic processes of some calcifying organisms in the China seas[36]. Calcifying organisms in the China seas could be of major ecological and economic importance. China is known as one of the most important countries of marine aquaculture industry. At year 2016, aquaculture production (excluding aquatic plants) from China is 4.97×10^7 t, accounting for about 61% of the global total aquaculture production, and large quantities of the marine aquaculture production are calcifying organisms[37]. Therefore, acidification in the China seas could lead to reductions in the aquaculture production and the consequent economic losses, meanwhile, posing threats to marine ecosystems.

For lack of historical observational data and the requirement for future projections in ocean chemistry fields, numerical models were used to investigate the changes in ocean acidification and biogeochemical processes in previous studies. For example, modeling studies show consistently that the drop in sea surface mean pH since preindustrial times is about 0.1[11,38,39], which is compared well with observational-based estimates[19]. By forcing the Lawrence Livermore National Laboratory ocean general-circulation model under IPCC SRES scenario, Caldeira and Wickett (2005) indicated that ocean surface pH could be reduced by 0.3–0.5 units by the end of this century[40]. By forcing 13 ocean-carbon cycle models under IPCC IS92a scenario, Orr *et al.* (2005) projected that surface seawater would be undersaturated with respect to aragonite in Mid-21st century[38].

In addition to the global scale, projections of future ocean acidification for specific spots of ocean in the East China are also provided in some other studies[41–44]. For example, Chou *et al.* reported that under the IPCC IS92a emission scenario, under the total effects of eutrophication and elevated atmospheric CO_2, the bottom water of the Yangtze River plume area would be undersaturated with respect to aragonite ($\Omega_A \approx 0.8$) by the end of this century, threatening the benthic ecosystem[43]. Zhai, using a predicted scenario that atmospheric CO_2 increases by 100 ppm for the 2050 s since present, proposed that half of the Yellow Sea benthos would be covered by acidified seawater having a critical Ω_A of less than 1.5[41]. In addition, under the IS92a scenario, Xu *et al.* proposed that by year 2100, surface seawater with $\Omega_A > 2.0$ would disappear over most of the ocean area in BoHai and Yellow seas of China[42].

Compared to other models that previous studies used, UVic ESCM (the University of Victoria Earth System Climate Model) as a coupled climate-carbon cycle model of intermediate complexity, could simulate climate and ocean chemistry fields in millennia timescales with lower computational expenses. Meanwhile, the UVic model could reasonably capture observed key variables in global climate[45], the ocean carbon cycle[46–48], and historical oceanic uptake of carbon and its isotopes[49]. Refer to Methods section for detailed descriptions of the UVic model.

In this study, we extend previous studies by using UVic model to quantify ocean acidification induced by anthropogenic CO_2 for ocean in the East China (115–130°E, 20–40°N). Usually, previous studies would only focus on analysing the changes in seawater acidity, e.g., seawater pH; this study further quantifies the impacts of changes in ocean chemistry (i.e., DIC, ALK, salinity and temperature) on ocean acidification, as well as analyses the spatial heterogeneity of ocean acidification. In addition, we investigate the effects of CO_2-induced warming on different ocean chemistry fields, and compare the strength of individual impacts of oceanic CO_2 uptake and CO_2-induced warming on ocean acidification, which was ignored by previous relevant studies. Furthermore, in this study, we analyse the nonlinearity relationship between atmospheric CO_2 scenario used and ocean acidification, which enable us to have a better estimate of the extent of ocean acidification in the East China under different CO_2 emission policies. We aim to further our understanding of the role played by accelerated anthropogenic CO_2 emissions in the carbon cycle of ocean in the East China, which is also important for reliable projections of future changes in marine biogeochemistry and ecosystem in west Pacific.

Results

To quantify the effect of increasing atmospheric CO_2 concentration on ocean acidification in the East China, a series of 500-year Earth system model simulations are designed. From year 1800 to 2017, all model simulations are forced by observational-based atmospheric CO_2 concentration. After 2017, simulations are forced by Representation Concentration Pathway scenarios (RCPs, including RCP2.6, RCP4.5, RCP6.0, and RCP8.5) and

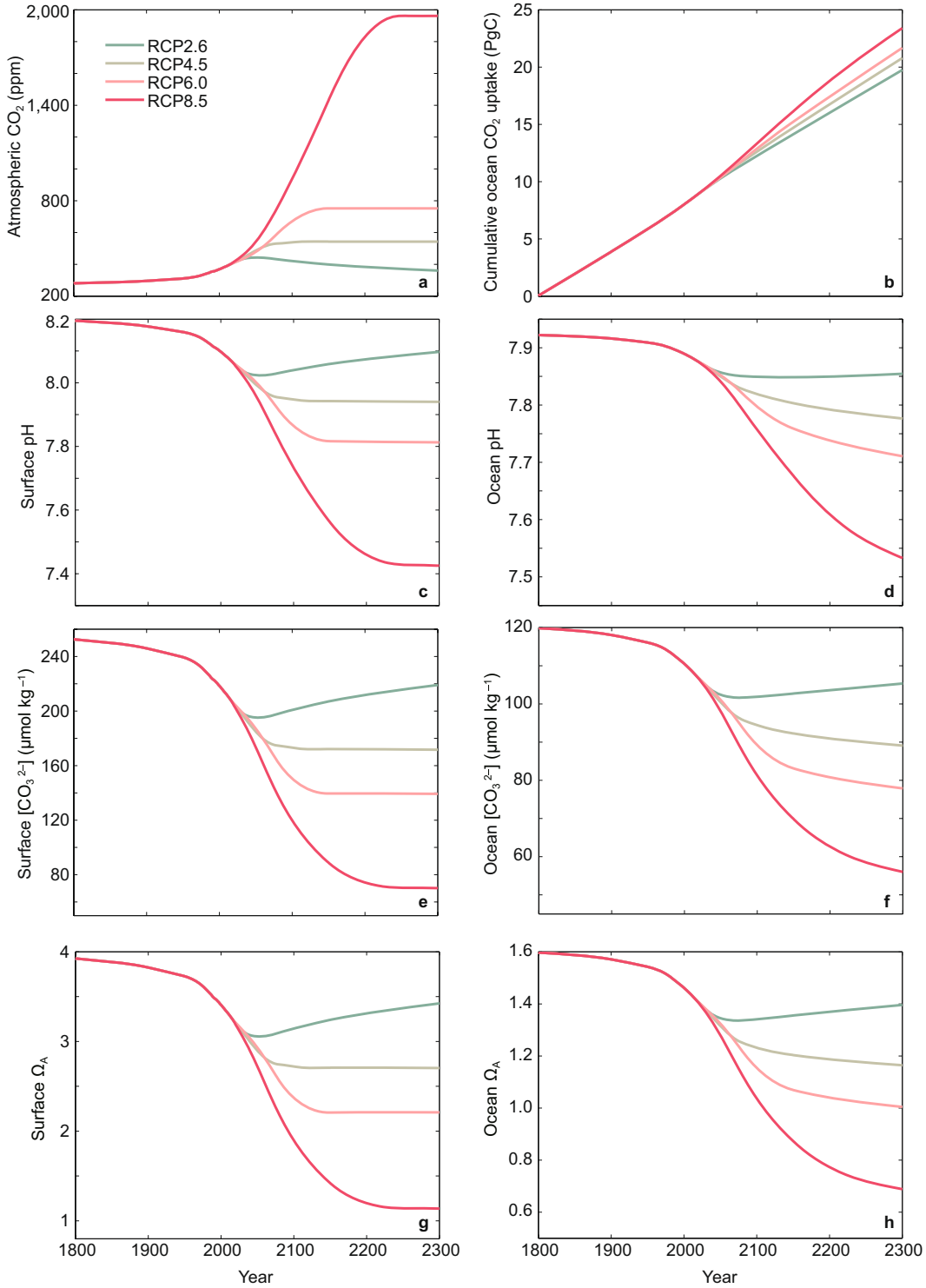

Figure 1. (**a**) Prescribed atmospheric CO_2 concentration and model-simulated time series of annual mean variable of (**b**) cumulative ocean CO_2 uptake, (**c**) ocean surface pH, (**d**) ocean mean pH, (**e**) ocean surface $[CO_3^{2-}]$, (**f**) ocean mean $[CO_3^{2-}]$, (**g**) ocean surface Ω_A, (**h**) ocean mean Ω_A in the East China. Results are shown for the four simulations using the four RCP scenarios depicted in Methods section.

their extensions up to year 2300 (Fig. 1a). To quantify the influences of CO_2-induced warming on ocean acidification in the East China, we conducted an additional set of simulations in which CO_2-induced warming is not allowed to affect the ocean carbon cycle. Refer to Methods section for detailed descriptions of the model and simulation experiments.

In the following, we first present results from the simulations including CO_2-induced warming effects on the ocean carbon cycle. Then, in the "Impacts of CO_2-induced warming on ocean acidification in the East China"

	UVic ESCM	IPCC AR5
Preindustrial-2011 cumulative (PgC)	147	155 ± 30
1980–1989 average (PgC yr^{-1})	1.8	2.0 ± 0.7
1990–1999 average (PgC yr^{-1})	2.0	2.2 ± 0.7
2000–2009 average (PgC yr^{-1})	2.3	2.3 ± 0.7
2002–2011 average (PgC yr^{-1})	2.4	2.4 ± 0.7

Table 1. Model-simulated global oceanic CO_2 uptake compared with observational-based estimates reported in IPCC AR5, which show uncertainties as 90% confidence intervals[8]. Shown in the table are the accumulated oceanic CO_2 uptake during preindustrial time-year 2011, and averaged oceanic CO_2 uptake during the 1980s, 1990s, 2000s, and the decade since 2002.

section, by comparing the results from simulations with and without CO_2-induced warming, we analyse the effects of CO_2-induced warming on ocean acidification in the East China.

Model evaluation. UVic-simulated global oceanic CO_2 uptake during the historical period since preindustrial time is consistent with observational-based estimates reported by IPCC AR5[8] (Table 1). For example, simulated cumulative oceanic CO_2 uptake during preindustrial time-year 2011 is 147 PgC, within the observational range of 155 ± 30 PgC reported by IPCC AR5[8] (Table 1). Model-simulated averaged oceanic CO_2 uptake during 2002–2011 is 2.4 PgC yr^{-1}, which compares well with the observed value of 2.4 ± 0.7 PgC yr^{-1} (Table 1). Model-simulated atmospheric CO_2 concentration is also consistent with observations. For example, simulated annual mean atmospheric CO_2 concentration at year 2017 is 405.0 ppm (Fig. 1a), compared well with observational-based estimate of 405.0 ± 0.1 ppm[1].

Model-simulated carbon-related tracers are also compared with observed estimates from the Global Ocean Data Analysis Project (GLODAP)[50]. As shown in Supplementary Fig. S1, simulated vertical profiles of dissolved inorganic carbon (DIC) and alkalinity (ALK) for ocean in the East China agree well with observational-based estimates. In addition, the UVic model can capture the observed large-scale distributions of key tracers for the global ocean, as well as different ocean basins (refer to Supplementary Material of Cao *et al.*[48]).

Ocean acidification in the East China: historical conditions since preindustrial time. Under the CO_2 concentration scenario depicted in Fig. 1a and Supplementary Fig. S2a, by year 2017, the atmospheric CO_2 concentration increases to 404 ppm (see Supplementary Table S1). With the increasement in atmospheric CO_2 concentration, the ocean continuously absorbs anthropogenic CO_2 from the atmosphere, leading to acidification in the global ocean (see Supplementary Fig. S3). As shown in Fig. S3, generally, the mid-latitude ocean surface shows greater decreases in pH, $[CO_3^{2-}]$ and Ω_A than the tropical and high latitude ocean surface.

As part of the mid-latitude ocean, ocean surface in the East China suffers greater acidification relative to sea surface in low and high latitudes from preindustrial time to year 2017. For example, by year 2017, sea surface mean pH in the high and low latitudes both dropped by 0.11 units, while sea surface pH in the East China dropped by 0.13 units, corresponding to a 35% rise in $[H^+]$ (Fig. 1c, Supplementary Figs. S2b, S3a and Table S1). Over the same time period, sea surface mean $[CO_3^{2-}]$ in the low latitudes reduced by 16%, contrasted to reductions by 18% for ocean in the East China (Fig. 1e, Supplementary Fig. S3b, and Table S1). This study will focus on analysing ocean acidification conditions in the East China (unless otherwise stated), in which ecosystems could be especially vulnerable to ocean acidification, triggering important effects on global fishery and marine aquaculture industries.

Figs. 2 and 3 show the simulated spatial distributions of the trend in ocean acidification in the East China from 1800 to 2017. Surface pH in the Yellow Sea shows a greater decrease relative to rest of the ocean in the East China, where surface $[CO_3^{2-}]$ and Ω_A reduce less. The different spatial distributions of the trends in ocean surface pH, $[CO_3^{2-}]$ and Ω_A are mainly due to different thermodynamic dependence of pH and $[CO_3^{2-}]$ on temperature[32]. With the growth in atmospheric CO_2 content, the ocean's continuous absorption of CO_2 leads to the exacerbation of ocean acidification with faster speed (Fig. 3). For instance, simulated results show the reductions in sea surface pH are faster in the last 20 years (years 2000–2009 and 2010–2017) relative to years 1980–1999 (Fig. 3f,h, Supplementary Fig. S2b).

Changes in seawater acidity in the East China mainly result from CO_2-induced changes in ocean DIC, ALK, salinity and temperature (Fig. 4, refer to Methods section for detailed descriptions of the analysis of ocean chemistry fields). As shown in Figs. 4 and 5, the decreases of sea surface pH, $[CO_3^{2-}]$ and Ω_A are largely a result of rising surface DIC, driven by the continuous oceanic CO_2 uptake. For example, by year 2017, the increase of sea surface DIC accounting for 82%, 94%, and 96% of the reductions of surface pH, $[CO_3^{2-}]$ and Ω_A, respectively (Fig. 4). The rising temperature due to global warming have different influences on sea surface pH and Ω_A, mainly as a result of different thermodynamic dependences of these two variables on temperature. For instance, by year 2017, the rising temperature accounting for 13% and −4% of the decreases in sea surface pH and Ω_A, respectively (Figs. 4 and 5). The reduction in sea surface alkalinity is mainly due to changes in ocean $CaCO_3$ cycles, adding to the reductions in surface pH, $[CO_3^{2-}]$ and Ω_A (Figs. 4 and 5). Changes in sea surface salinity are relatively small and the effects of surface salinity changes on ocean acidification are nearly negligible (Figs. 4 and 5).

Different spatial distributions of changes in sea surface DIC, ALK, salinity and temperature could have implications for the distributions of changes in surface pH, $[CO_3^{2-}]$ and Ω_A[17,48]. For example, surface pH in the Yellow Sea shows a greater decrease (1800–2017) relative to the rest of ocean in the East China, which is largely due to the

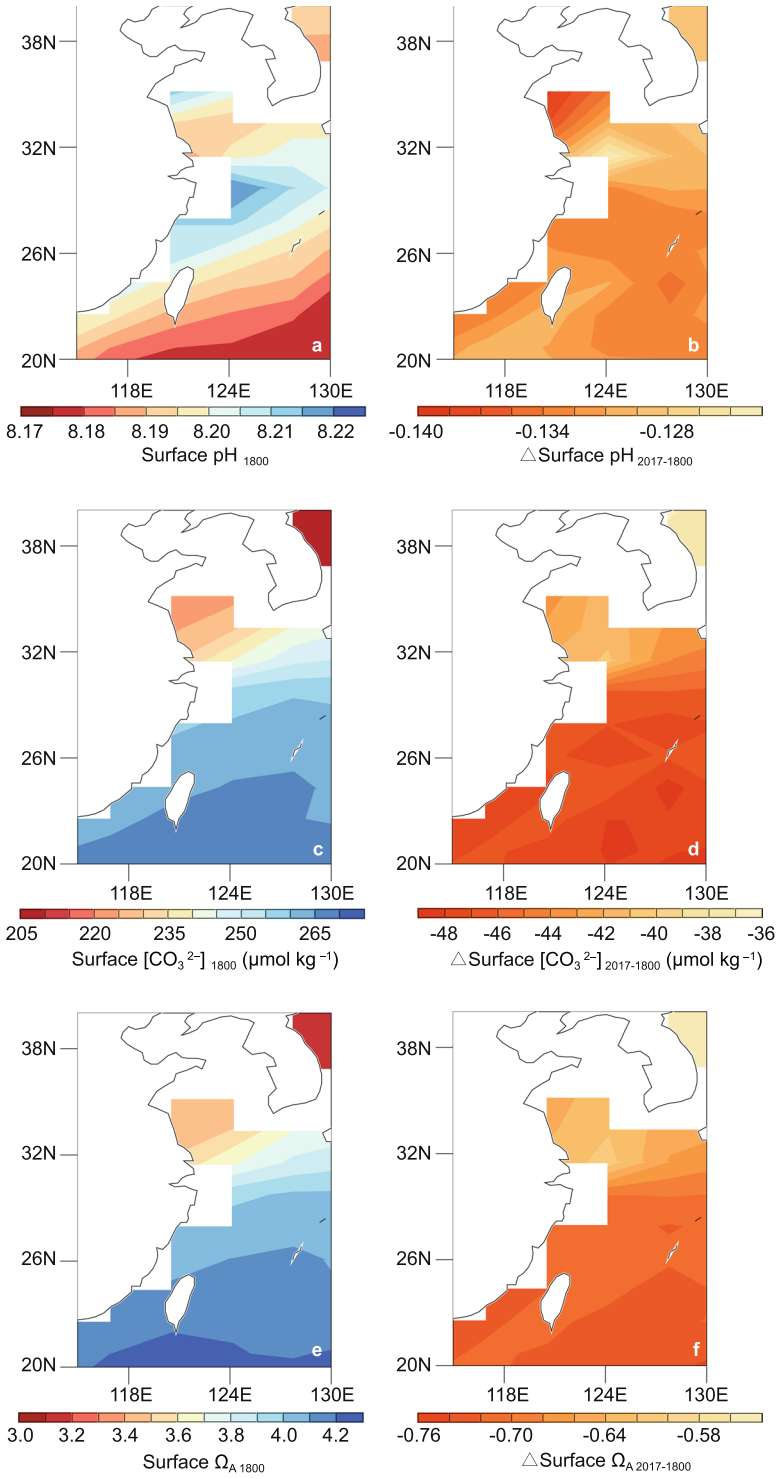

Figure 2. Spatial distributions of simulated ocean surface (**a**,**b**) pH, (**c**,**d**) $[CO_3^{2-}]$, and (**e**,**f**) Ω_A in the East China. Results shown in (**a**,**c**,**e**) are for year 1800 and (**b**,**d**,**f**) are for the changes at year 2017 relative to 1800. The figures are generated using UV-CDAT version 2.5.0 (http://uvcdat.llnl.gov/).

rapid elevation in surface temperature, while surface DIC and ALK over the Yellow Sea does not show relatively significant trends (Fig. 2b, Supplementary Fig. S4).

In previous projects and studies, observational-based estimates of ocean acidification for specific areas in the East China have also been reported. For instance, field surveys conducted by Zhai at years 2012, 2015 and 2016, showing acidified seawaters with critical Ω_A of less than 1.5 in the Yellow Sea[41]. Whereas in our simulated results, ocean mean Ω_A (2012–2016 average) in the East China is about 1.4, consistent with the data-based estimates from Zhai (2018). In addition, based on a survey conducted at year 2013, Xu *et al.* concluded that surface Ω_A in

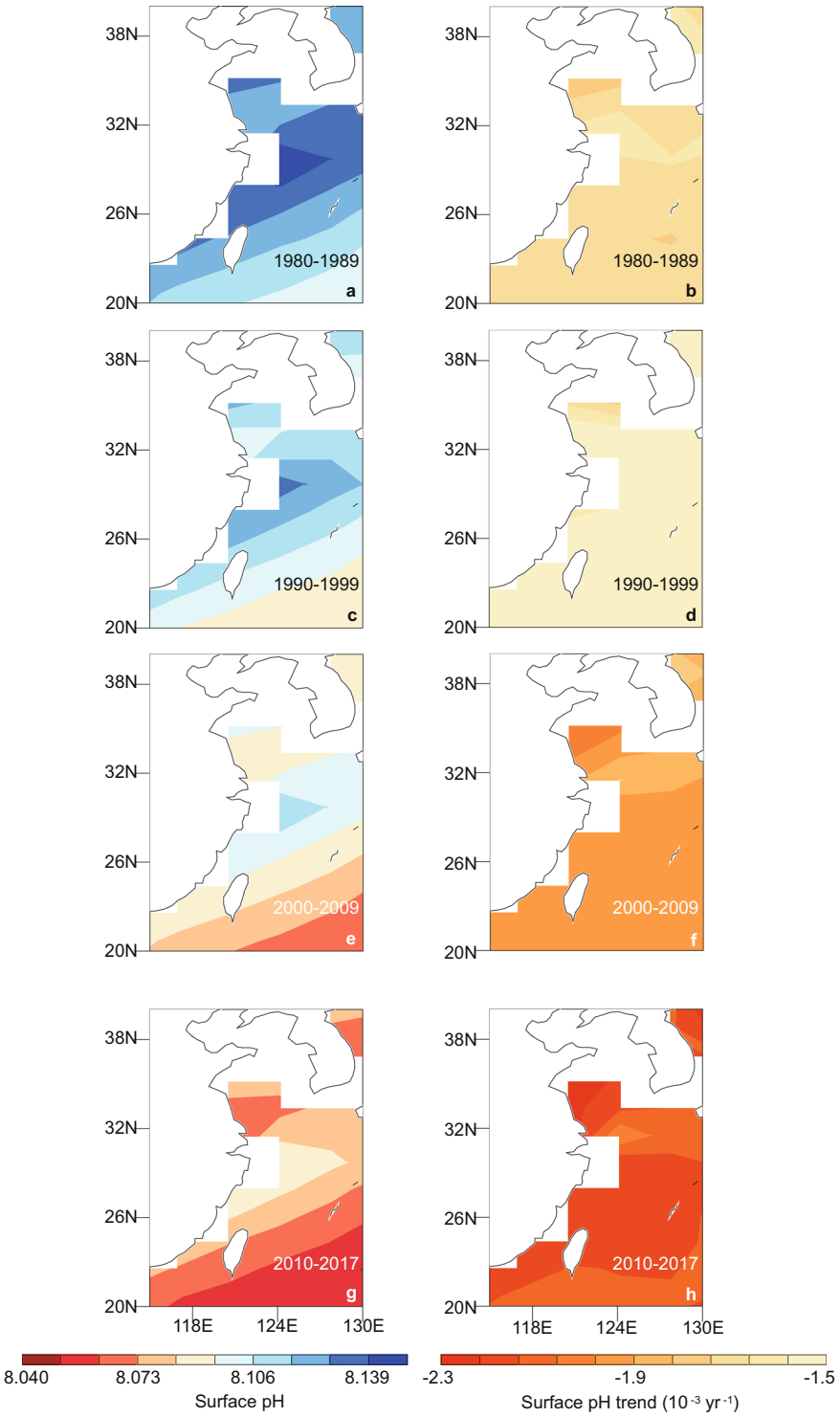

Figure 3. Spatial distributions of simulated (**a**,**c**,**e**,**g**) decadal mean and (**b**,**d**,**f**,**h**) decadal mean trend of ocean surface pH in the East China. Results are shown for years (**a**,**b**) 1980–1989, (**c**,**d**) 1990–1999, (**e**,**f**) 2000–2009, (**g**,**h**) 2010–2017, respectively. The figures are generated using UV-CDAT version 2.5.0 (http://uvcdat.llnl.gov/).

BoHai and Yellow seas ranged from 2.0 to 3.8[42], which compares well with our sea surface mean Ω_A of 3.3 in the East China.

Future projections of ocean acidification in the East China. To have a better understanding of the ocean acidification conditions in the East China under different atmospheric CO_2 scenarios, we performed four simulations under different RCP scenarios (Fig. 1a). With the continuous increasement in atmospheric CO_2

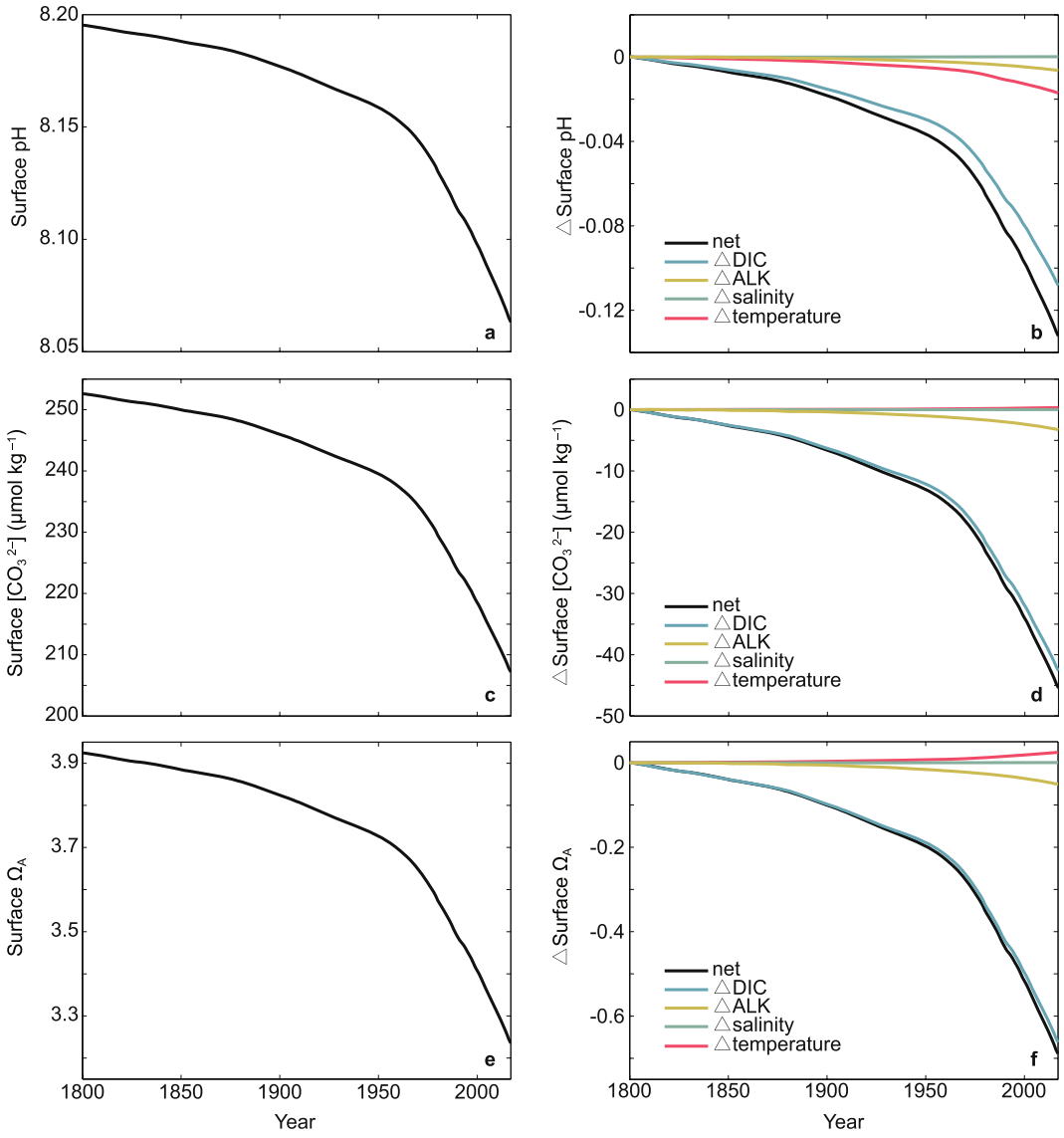

Figure 4. Time series of simulated ocean surface (**a**,**b**) pH, (**c**,**d**) $[CO_3^{2-}]$, and (**e**,**f**) Ω_A in the East China from year 1800 to 2017. Results shown in (**a**,**c**,**e**) are for annual mean, and (**b**,**d**,**f**) are for the individual effects of changes in dissolved inorganic carbon (DIC), alkalinity (ALK), salinity and temperature on the corresponding fields.

content, the ocean keeps absorbing atmospheric CO_2, leading to continuing acidification in the global ocean (see Supplementary Figs. S5 and S6). As shown in Figs. S5 and S6, in terms of $[CO_3^{2-}]$ and Ω_A, ocean surface in the East China would experience greater ocean acidification than the tropical and high latitude ocean surface. The Arctic Ocean experiences the greatest reductions in sea surface pH, mainly due to the effects of rising temperature (Fig. 4b).

Simulated results show that responses of ocean acidification could be sensitive to the atmospheric CO_2 scenarios used. For example, in the simulation under RCP2.6 scenario, by year 2300, the cumulative CO_2 uptake for ocean in the East China is 19.7 PgC, leading to reductions in sea surface pH and $[CO_3^{2-}]$ by 1% and 13% (Fig. 1, Supplementary Table S1). In contrast, in the simulation under RCP8.5 scenario, by year 2300, the cumulative oceanic CO_2 uptake is 23.4 PgC, resulting in reductions in surface pH and $[CO_3^{2-}]$ by 9% and 72%, respectively (Fig. 1, Supplementary Table S1).

In addition, the relationship between atmospheric CO_2 scenario used and ocean acidification in the East China is nonlinear (Fig. 6). For instance, at year 2300, for sea surface pH in the East China, $\Delta pH_{RCP8.5\text{-}RCP6.0}/\Delta CO_{2\,RCP8.5\text{-}RCP6.0} = -3.2 \times 10^{-3}$, $\Delta pH_{RCP6.0\text{-}RCP4.5}/\Delta CO_{2\,RCP6.0\text{-}RCP4.5} = -6.1 \times 10^{-3}$, while $\Delta pH_{RCP4.5\text{-}RCP2.6}/\Delta CO_{2\,RCP4.5\text{-}RCP2.6} = -8.6 \times 10^{-3}$ (Fig. 6, Table S1), indicating faster acidification rates under scenarios of lower atmospheric CO_2 content. At year 2300, for sea surface $[CO_3^{2-}]$ in the East China, $\Delta[CO_3^{2-}]_{RCP8.5-RCP6.0}/\Delta CO_{2\,RCP8.5\text{-}RCP6.0} = -0.06$, $\Delta[CO_3^{2-}]_{RCP6.0-RCP4.5}/\Delta CO_{2\,RCP6.0\text{-}RCP4.5} = -0.15$, while $\Delta[CO_3^{2-}]_{RCP4.5-RCP2.6}/\Delta CO_{2\,RCP4.5\text{-}RCP2.6} = -0.26$ (Fig. 6, Table S1), showing greater nonlinearity than surface pH. The nonlinearity between

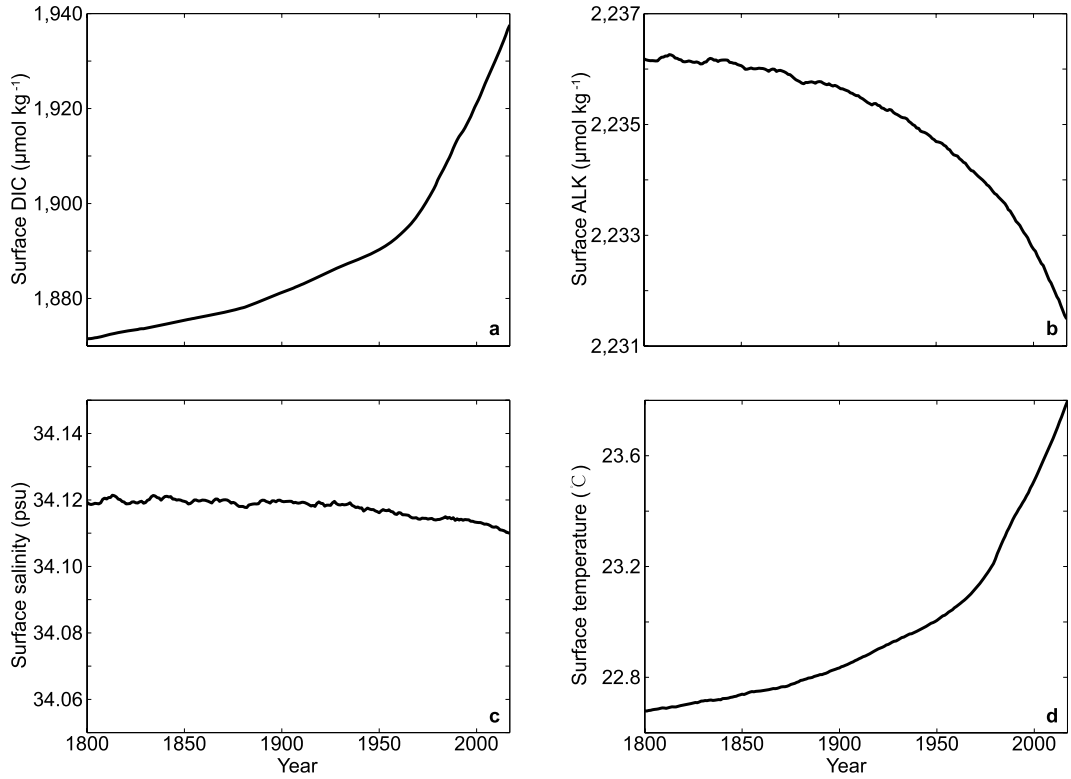

Figure 5. Time series of simulated annual mean ocean surface (**a**) dissolved inorganic carbon (DIC), (**b**) alkalinity (ALK), (**c**) salinity, (**d**) temperature in the East China from year 1800 to 2017.

atmospheric CO_2 scenario used and ocean acidification is noteworthy, which hints that if we aim to mitigate ocean acidification in the East China under a scenario of high atmospheric CO_2 content, a deeper reduction of anthropogenic CO_2 emission may be needed.

With the decrease of seawater $[CO_3^{2-}]$ in the East China, the aragonite saturation state (Ω_A) would also diminish (Fig. 1g,h). We take the simulations under RCP8.5 and RCP4.5 scenarios for example, to investigate the possible effects of ocean acidification on seawater chemistry in the East China under intensive and medium atmospheric CO_2 scenarios.

Under RCP8.5, due to the oceanic CO_2 uptake and the resultant reduction in $[CO_3^{2-}]$, ocean Ω_A drops from the preindustrial value of 1.6 to 0.7 by year 2300, and seawater Ω_A would become less than 1 at nearly all ocean depths (Fig. 1h, Supplementary Fig. S7a and Table S1). The decreases in seawater Ω_A would pose threats to calcifying organisms over ocean in the East China. For example, seawater that surrounding coral reefs becomes more and more acidic, from surface to depth (see Supplementary Figs. S7a, and S8a–c). Aragonite is the main constituents of calcareous endoskeleton of corals, therefore, the corals surrounded by undersaturated seawater with respect to aragonite ($\Omega_A < 1$) would encounter adverse impacts. There are also intriguing evidences that even in supersaturated seawater, $CaCO_3$ also dissolves[3,51]. Seawater chemistry fields at different depths have different responses to oceanic CO_2 uptake. For ocean in the East China, by year 2100, the reduction in Ω_A is 2.0 at depth of 17.5 m, which becomes 0.3 at depth of 642.5 m (see Supplementary Fig. S7a). Changes in ocean chemistry at depths lag behind changes in the surface ocean because of the long time scale associated with the penetration of CO_2 into the deep ocean.

In comparison, in the simulation under RCP4.5 scenario, ocean Ω_A drops from the preindustrial value of 1.6 to 1.2 by year 2300 (Fig. 1h, Supplementary Table S1). Compared with simulated results under RCP8.5, simulation under RCP4.5 presents higher ocean Ω_A at years 2100 and 2300 (see Supplementary Figs. S7 and S8). In addition, from year 2100 to 2300, in simulation under RCP8.5, Ω_A at different depths continues to decrease, while in simulation under RCP4.5, the reductions in Ω_A at different depths, especially the decreases in surface Ω_A are slight (Fig. 1, Supplementary Figs. S7 and S8). Therefore, responses of ocean acidification in the East China would be sensitive to the changes in atmospheric CO_2, demonstrating the important impacts of atmospheric CO_2 changes on marine chemistry.

Impacts of CO_2-induced warming on ocean acidification in the East China. The impact of CO_2-induced warming on ocean acidification in the East China could be inspected by comparing modeled ocean chemistry fields from simulations with and without CO_2-induced warming (see Supplementary Table S2 and Fig. S9). Generally, CO_2-induced warming would decrease the amount of ocean uptake of atmospheric CO_2, mitigating ocean acidification (see Supplementary Table S2). Previous studies concluded that, this warming-induced reduction in oceanic CO_2 uptake is mainly as a result of warming-induced decreases in CO_2 solubility and ocean

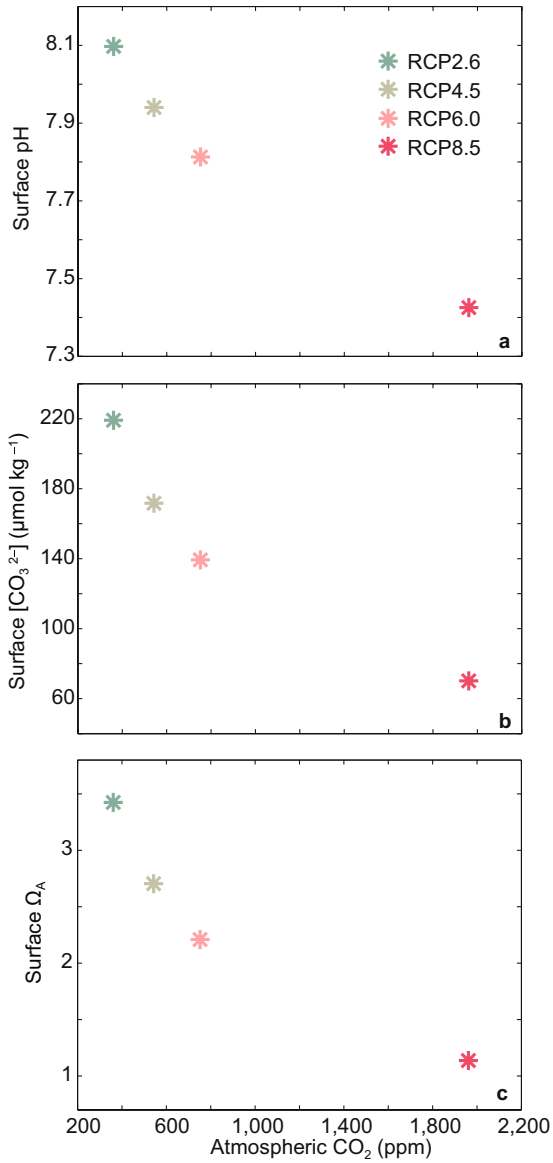

Figure 6. Prescribed atmospheric CO_2 concentration against model-simulated ocean surface (**a**) pH, (**b**) $[CO_3^{2-}]$, and (**c**) Ω_A in the East China at year 2300. Results are shown for the four simulations using the four RCP scenarios depicted in Methods section, revealing the nonlinearity relationship between atmospheric CO_2 scenario used and ocean acidification.

ventilation (ocean mixing and circulation)[9,52,53]. Effects of warming-induced changes in ocean biology processes (including phytoplankton growth and mortality rates, and detritus remineralization) offset with each other, therefore the total warming-induced biological impact on oceanic CO_2 uptake and ocean acidification is small (refer to Cao and Zhang, 2017)[9].

For regional ocean in the East China, the responses of seawater pH and $[CO_3^{2-}]$ to CO_2-induced warming are different (Fig. 7). The decoupled effects of CO_2-induced warming on pH and $[CO_3^{2-}]$ are mainly due to their different thermodynamic dependence on temperature[39] (Fig. 4). For pH, the direct effect of rising temperature tends to reduce seawater pH (Fig. 4b), while warming-induced reductions in CO_2 solubility and ocean ventilation would suppress oceanic CO_2 uptake and mitigate the decrease in ocean pH. Total influence of CO_2-induced warming on seawater pH mainly depends on the relative importance of these two effects, i.e., thermodynamic effects of temperature increasing and warming-induced reductions in CO_2 solubility and ocean ventilation. For ocean in the East China, relative to ocean depths, changes of pH in the ocean surface depend more on thermodynamic effects of rising temperature, resulting in decreased surface pH due to CO_2-induced warming (Fig. 7a). At ocean depths, at year 2100, pH changes depend more on warming-induced reductions in CO_2 solubility and ocean ventilation, leading to increased ocean pH due to CO_2-induced warming (Fig. 7b). For instance, at year 2100, in simulation RCP4.5, for ocean in the East China, surface pH decreases by about 0.005 due to CO_2-induced warming, whereas ocean mean pH increases by 0.005 due to CO_2-induced warming (Fig. 7 and Table S2). For

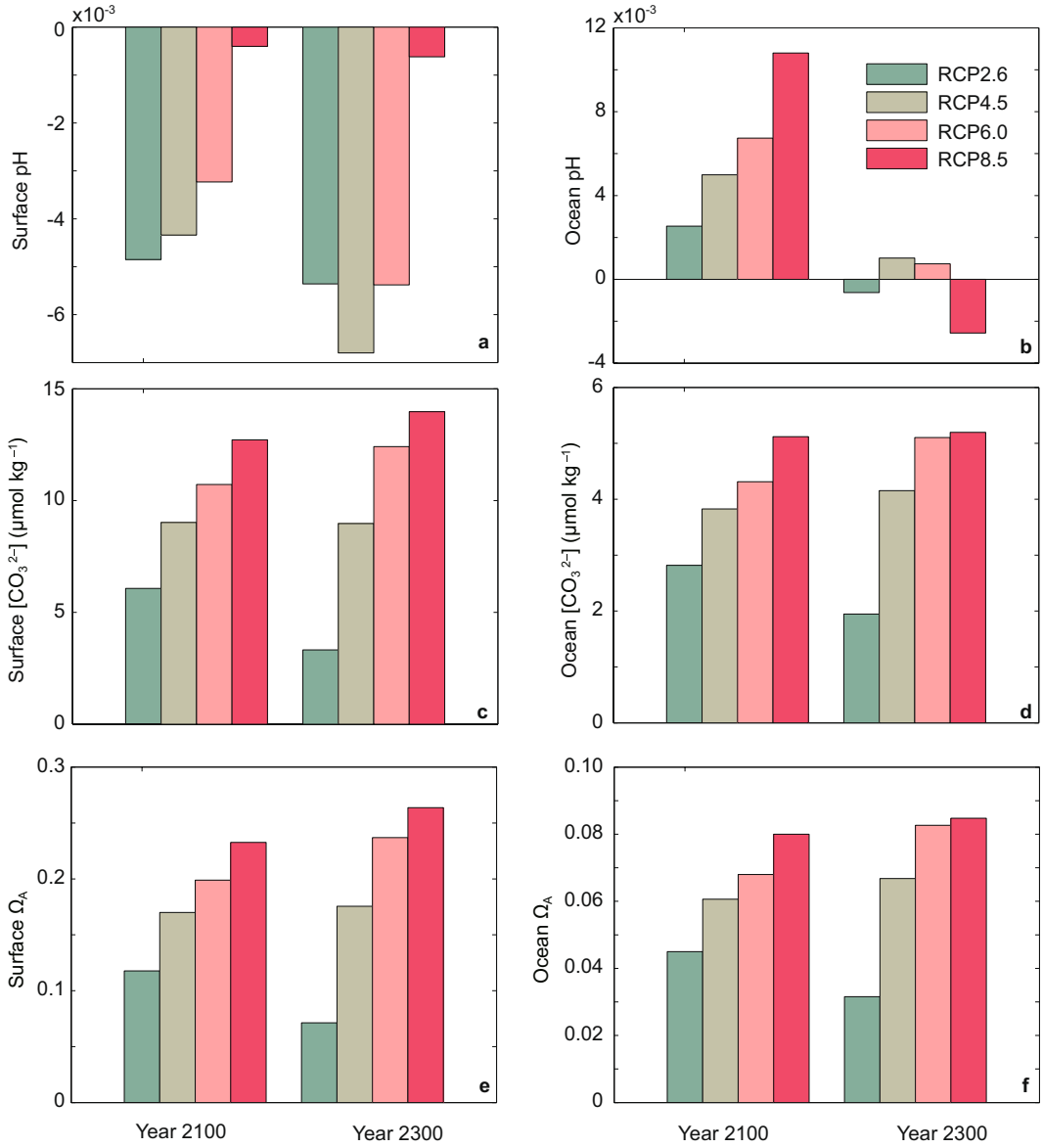

Figure 7. Model-simulated effects of CO_2-induced warming at years 2100 and 2300 on (**a**) ocean surface pH, (**b**) ocean mean pH, (**c**) ocean surface $[CO_3^{2-}]$, (**d**) ocean mean $[CO_3^{2-}]$, (**e**) ocean surface Ω_A, (**f**) ocean mean Ω_A in the East China. The effect of CO_2-induced warming is represented by the difference between the results from simulations with and without warming effect. Results are shown for the four simulations using the four RCP scenarios depicted in Methods section.

$[CO_3^{2-}]$ and Ω_A, thermodynamic effects of temperature increasing and warming-induced reductions in CO_2 solubility and ocean ventilation both act to mitigate the reductions in $[CO_3^{2-}]$ and Ω_A (Fig. 7c–f).

Compared to the individual effect of oceanic CO_2 uptake, the effect of CO_2-induced warming on ocean acidification in the East China is relatively small (see Supplementary Fig. S9). For instance, at year 2300, under RCP8.5, for ocean in the East China, CO_2-induced surface $[CO_3^{2-}]$ decrease is 196 μmol kg^{-1} ($\Delta[CO_3^{2-}]_{2300-1800}$ under RCP8.5 without warming effect), whereas warming-induced surface $[CO_3^{2-}]$ increase is only 14 μmol kg^{-1} (Fig. 7, and Supplementary Table S2, Fig. S9).

Discussion

In this study, we conduct model simulations to assess ocean acidification in the East China on the timescale of centuries. During preindustrial time-year 2017, under the atmospheric CO_2 scenario that is based on observations, as atmospheric CO_2 concentration increases, the global ocean experiences acidification, and the ocean surface in the East China is one of the most vulnerable areas to ocean acidification. By year 2017, sea surface pH in the East China drops from the preindustrial level of 8.20 to 8.06, corresponding to a 35% rise in $[H^+]$. In addition, the decrease rate of surface pH becomes faster in the last two decades. The changes in surface seawater acidity largely result from CO_2-induced changes in surface DIC, ALK, salinity and temperature, among which

DIC plays the most important role (accounting for more than 82% reductions in surface pH, $[CO_3^{2-}]$ and Ω_A). In future projections, responses of ocean acidification could be sensitive to the atmospheric CO_2 scenarios chosen. By year 2300, simulated reductions in sea surface $[CO_3^{2-}]$ are 13% under RCP2.6, 32% under RCP4.5, 45% under RCP6.0, contrasted to 72% under RCP8.5.

Moreover, our simulated results show that the relationship between atmospheric CO_2 scenario used and ocean acidification is nonlinear. This is important because if we want to mitigate ocean acidification in the East China under a scenario of high CO_2 concentration, a deeper reduction of anthropogenic CO_2 emission may be needed. Furthermore, our simulations show that with the continuous oceanic CO_2 uptake, changes in deep ocean chemistry exhibits time lag relative to the surface ocean, due to the long time scale associated with the slow penetration of excess CO_2 to the deep ocean. The long time scale for changes in deep ocean chemistry also indicates the urgent of deep reductions in anthropogenic CO_2 emissions, to avoid continuous accumulation of CO_2 at ocean depths. In addition, CO_2-induced warming acts to mitigate the reductions in seawater $[CO_3^{2-}]$ and Ω_A in the East China, and the individual effect of oceanic CO_2 uptake is much greater than the effect of CO_2-induced warming on ocean acidification.

Under RCP8.5, for ocean in the East China, by year 2300, with the decrease of ocean $[CO_3^{2-}]$, aragonite saturation state (Ω_A) would drop from its initial value of 1.6 to 0.7, and seawater Ω_A would become undersaturated ($\Omega_A < 1$) at nearly all ocean depths. Ocean in the East China is the habitat of numerous amounts of corals, fish, shellfish, and other calcifying organisms, such as crustaceans (e.g., penaeus, scylla serrata), gastropods (e.g., cypraea tigris, cassis cornuta), coccolithophorids (e.g., chrysophyta), including rare species. These calcifying organisms may not be able to acclimate to the reduction in seawater Ω_A. By carrying out short-term pCO_2/pH perturbation experiments, Wu and Gao concluded that, the combined impacts of seawater acidification and solar UV changes could also inhibit photosynthesis in the China seas[54]. Morphology, physiology and behavior of some other marine organisms (e.g., molluscs, cnidarians) could also be impacted by ocean acidification[55]. Therefore, ocean acidification in the East China could have adverse effects on fundamental biochemical processes and marine ecosystems. Since ocean in the East China plays an important role in global fishery and marine aquaculture industries, its trend in ocean acidification would have far-reaching consequences for the millions of people that depend on the food and other resources in the ocean for their livelihoods[56].

Our study has investigated the CO_2-induced ocean acidification conditions in the East China on timescales of centuries by using an Earth system model. Some processes or feedbacks that are not considered in this study may also have effects on ocean acidification[16,17,57]. For example, ocean acidification tends to suppress the calcification rate of some marine calcifying organisms, increasing surface ocean alkalinity and reducing seawater acidity[16]. This study also does not include the interactive feedbacks between ocean acidification and $CaCO_3$ in the sediments, which is considered to reduce the chemistry change extent in the deep ocean on timescales longer than a millennium[58–60].

In this study, based on model-simulated results, we diagnose ocean acidification in the East China during preindustrial time-year 2017, and highlight the potential future ocean acidification condition over timescales of centuries. Meanwhile, this study tries to provide useful information about the changes in future marine biogeochemical environment. Further observational and modeling studies would be required to develop a better understanding of the ocean carbon cycle and marine biogeochemistry, which is crucial for more reliable projections of future ocean acidification and its impacts on marine ecosystems.

Methods

Model description. In this study, we utilize the University of Victoria Earth System Climate Model (UVic ESCM) version 2.9, an intermediate complexity Earth system model[46]. The UVic model consists of an energy-moisture balance atmospheric model[61], a 3D ocean general circulation model[62], a thermodynamic/dynamic sea ice model[63,64], and ocean and land carbon cycle models[46,65–67]. The horizontal resolution of the UVic model is 1.8° (latitude) × 3.6° (longitude), which is similar to the resolutions of most coupled Atmosphere-Ocean General Circulation Models (AOGCMs)[45]. The ocean model of UVic is the Modular Ocean Model (MOM) version 2.2 with 19 vertical levels, developed by the Geophysical Fluid Dynamics Laboratory[62].

The ocean carbon cycle model of UVic comprises inorganic and organic carbon cycle modules. The inorganic carbon cycle is based on the Ocean Carbon-Cycle Model Intercomparison Project (OCMIP)[68]. The organic carbon cycle is represented by a nutrient-phytoplankton-zooplankton-detritus (NPZD) ocean ecosystem/biogeochemical model[46,67]. The land surface model and vegetation model are represented by Met Office Surface Exchange Scheme (MOSES) and Top-down Representation of Interactive Foliage and Flora Including Dynamics (TRIFFID) vegetation model, developed by the Hadley Center[65,66].

The UVic model has participated in a series of international model intercomparison projects, including an intercomparison of Earth System Models of Intermediate Complexity (EMICs) undertaken in support of the Intergovernmental Panel on Climate Change Fifth Assessment Report (IPCC AR5)[69,70], the Coupled Carbon Cycle Climate Model Intercomparison Project (CMIP)[71], the Paleoclimate Modeling Intercomparison Project (PMIP)[72], and a few thermohaline circulation experiments[73,74]. The UVic model has been widely used in the studies concerning future evolutions of the ocean biogeochemical cycles[46], interactions between global carbon cycle and climate change[71], and projections of ocean acidification[75,76].

The UVic model also has been widely used to investigate spatial distributions of physical and biogeochemical fields in both paleo and contemporary climate studies. For instance, Alexander *et al.* (2015) conducted model simulations with the UVic model and suggested that the spatial changes in carbonate dissolution during the Palaeocene-Eocene Thermal Maximum (PETM) could be explained by corrosive deep water spreading from the North Atlantic Ocean[77]. Bralower *et al.* (2014) found that UVic-simulated temperature, salinity, calcite saturation state, and dissolved O_2 and PO_4 at different ocean depths are generally agree with integrated published data from

the onset of the PETM at a coastal Site 690, Maud Rise in the Southern Ocean[78]. Xiao *et al.* (2012) used the UVic model to examine contributions of different climate forcings to surface air temperature over East China in the past millennium, and found the model successfully reproduced the observational-based temperature variation of East China[79]. Xiao *et al.* (2012) also suggested that the mean error of air temperature simulated by the UVic model could be even smaller than that by many famous complex models[45,79]. In addition, Meissner[80], Weaver *et al.*[81], Spence and Weaver[82], and Muglia and Schmittner[83] conducted UVic simulations to investigate variations in Atlantic meridional overturning circulation. Therefore, it is feasible to use the UVic model to quantify ocean acidification in the East China induced by oceanic uptake of anthropogenic CO_2 on timescales of centuries.

Simulation experiments. The UVic model was first spun up for 10,000 model years with a fixed preindustrial CO_2 concentration of 280 ppm to reach a quasi-equilibrium state of carbon cycle and climate system. Then, using this preindustrial state as an initial condition for the calendar year of 1800, two sets of four 500-year transient simulations are performed (i.e., from year 1800 to 2300). In the first set of simulations, rising atmospheric CO_2 concentration affects both the ocean carbon cycle and atmospheric radiation. While in the second set of simulations, rising atmospheric CO_2 concentration is not allowed to affect atmospheric radiation, that is, the ocean carbon cycle would not be impacted by CO_2-induced warming. Each set of experiments include four simulations. From year 1800 to 2017, atmospheric CO_2 concentration data are taken from observational-based estimates, and after 2017, CO_2 concentrations are taken from the Representation Concentration Pathway scenarios (RCPs) and their extensions up to year 2300[84] (Fig. 1a). The four scenarios used are RCP2.6, RCP4.5, RCP6.0, and RCP8.5, based on different mitigation policies for greenhouse gases[84,85]. The numbers after "RCP" represent that by year 2100, the radiative forcing reaches 2.6, 4.5, 6.0, or 8.5 $W\,m^{-2}$, respectively. Refer to Meinshausen *et al.* (2011) for detailed descriptions of these RCP scenarios[84].

Analysis of ocean chemistry fields. In this study, we calculate ocean carbonate chemistry fields, including seawater pH, $[CO_3^{2-}]$ and Ω_A, based on equations from the OCMIP-3 project (http://ocmip5.ipsl.jussieu.fr/OCMIP/). We use UVic-simulated ocean temperature, salinity, DIC, ALK, and observational-based estimates of ocean phosphate and silicate concentrations from the Global Ocean Data Analysis Project (GLODAP)[50]. Here comes the calculations[86].

Thermodynamic carbonate chemistry system can be generally represented by the following 6 variables: $[H^+]$, DIC, ALK, $[CO_2]$, $[HCO_3^-]$, and $[CO_3^{2-}]$. Here, $[CO_2]$ is the sum of concentrations of CO_2 (aq) (aqueous carbon dioxide) and H_2CO_3 (carbonate acid), and $[HCO_3^-]$ represents bicarbonate ion concentration. Additionally, equilibrium expressions for H_2CO_3 dissociation are given by

$$K_1^* = \frac{[HCO_3^-][H^+]}{[CO_2]} \tag{3}$$

$$K_2^* = \frac{[CO_3^{2-}][H^+]}{[HCO_3^-]} \tag{4}$$

Expressions for DIC and ALK are given by

$$DIC = [CO_2] + [HCO_3^-] + [CO_3^{2-}] \tag{5}$$

$$ALK \approx [HCO_3^-] + 2[CO_3^{2-}] + [OH^-] - [H^+] \tag{6}$$

Based on the above 6 variables ($[H^+]$, DIC, ALK, $[CO_2]$, $[HCO_3^-]$, and $[CO_3^{2-}]$), and 4 equations (Eqs. (3–6)) of ocean carbonate chemistry, given 2 known variables, we can calculate the rest 4 variables[87]. Therefore, changes in temperature, salinity (temperature and salinity changes would affect K_1^* and K_2^*), DIC, and ALK, would result in changes in pH ($pH = -\log_{10}[H^+]$) and $[CO_3^{2-}]$, i.e., changes in seawater acidity.

Data availability

All data generated or analysed during this study are included in this published article (and its Supplementary Information files).

Received: 5 August 2019; Accepted: 20 November 2019;
Published online: 06 December 2019

References

1. Dlugokencky, E. & Tans, P. Trends in atmospheric carbon dioxide. National Oceanic & Atmospheric Administration, Earth System Research Laboratory (NOAA/ESRL), [2019-3], http://www.esrl.noaa.gov/gmd/ccgg/trends/global.html (2019).
2. Le Quéré, C. *et al.* Global carbon budget 2018. *Earth syst sci data.* **10**(4), 2141–2194 (2018).
3. Sarmiento, J. L. & Gruber, N. *Ocean Biogeochemical Dynamics.* (Princeton University Press, Princeton and Oxford, 2006).
4. Ren, G., Ding, Y. & Tang, G. An overview of mainland China temperature change research. *J Meteorol Res-Prc.* **31**(1SI), 3–16 (2017).
5. Lin, L., Gettelman, A., Fu, Q. & Xu, Y. Simulated differences in 21st century aridity due to different scenarios of greenhouse gases and aerosols. *Climatic Change.* **146**(3–4SI), 407–422 (2018).
6. Zhu, Z. & Li, T. Extended-range forecasting of Chinese summer surface air temperature and heat waves. *Clim dynam.* **50**(5–6), 2007–2021 (2018).
7. Zhou, T. J. *et al.* Weak response of the Atlantic thermohaline circulation to an increase of atmospheric carbon dioxide in IAP/LASG climate system model. *Chinese Science Bulletin.* **50**(6), 592–598 (2005).

8. Ciais, P. *et al*. Carbon and Other Biogeochemical Cycles in *Climate Change 2013: The Physical Science Basis*. *Contribution of Working Group I to the Fifth Assessment Report of the Intergovernmental Panel on Climate Change* (ed. Stocker, T. F. *et al*.) 486 (Cambridge University Press, Cambridge, United Kingdom and New York, NY, USA, 2013).
9. Cao, L. & Zhang, H. The role of biological rates in the simulated warming effect on oceanic CO_2 uptake. *J Geophys Res-Biogeo.* **122**(5), 1098–1106 (2017).
10. Yuan, W. *et al*. Differentiating moss from higher plants is critical in studying the carbon cycle of the boreal biome. *Nat Commun.* **5**(8), 4270 (2014).
11. Caldeira, K. & Wickett, M. E. Anthropogenic carbon and ocean pH. *Nature.* **425**(6956), 365 (2003).
12. Strong, A. L., Kroeker, K. J., Teneva, L. T., Mease, L. A. & Kelly, R. P. Ocean acidification 2.0: Managing our changing coastal ocean chemistry. *Bioscience.* **64**(7), 581–592 (2014).
13. Mongin, M. *et al*. The exposure of the Great Barrier Reef to ocean acidification. *Nat Commun.* **7**(1), 10732 (2016).
14. Koweek, D. A. *et al*. Expected limits on the ocean acidification buffering potential of a temperate seagrass meadow. *Ecol Appl.* **28**(7), 1694–1714 (2018).
15. Raymond, P. A. & Hamilton, S. K. Anthropogenic influences on riverine fluxes of dissolved inorganic carbon to the oceans. *Limnol Oceanogr.* **3**, 143–155 (2018).
16. Zhang, H. & Cao, L. Simulated effect of calcification feedback on atmospheric CO_2 and ocean acidification. *Sci Rep-UK.* **6**, 20284 (2016).
17. Zhang, H. & Cao, L. Simulated effects of interactions between ocean acidification, marine organism calcification, and organic carbon export on ocean carbon and oxygen cycles. *Sci China Earth Sci.* **61**(6), 804–822 (2018).
18. Hofmann, M. & Schellnhuber, H. J. Oceanic acidification affects marine carbon pump and triggers extended marine oxygen holes. *P Natl Acad Sci USA.* **106**(9), 3017–3022 (2009).
19. Stocker, T. F. *et al*. The Physical Science Basis in *Climate Change 2013: Contribution of Working Group I to the Fifth Assessment Report of the Intergovernmental Panel on Climate Change* (Cambridge University Press, Cambridge, United Kingdom and New York, NY, USA, 2013).
20. Royal Society. *Ocean acidification due to increasing atmospheric carbon dioxide*. (The Royal Society, London, 2005).
21. Feely, R. A. *et al*. Impact of anthropogenic CO_2 on the $CaCO_3$ system in the oceans. *Science.* **305**(5682), 362–366 (2004).
22. Gattuso, J. P., Frankignoulle, M., Bourge, I., Romaine, S. & Buddemeier, R. W. Effect of calcium carbonate saturation of seawater on coral calcification. *Global Planet Change.* **18**(1), 37–46 (1998).
23. Langdon, C. *et al*. Effect of calcium carbonate saturation state on the calcification rate of an experimental coral reef. *Global Biogeochem Cy.* **14**(2), 639–654 (2000).
24. Zondervan, I., Zeebe, R. E., Rost, B. & Riebesell, U. Decreasing marine biogenic calcification: A negative feedback on rising atmospheric pCO_2. *Global Biogeochem Cy.* **15**(2), 507–516 (2001).
25. Riebesell, U. *et al*. Reduced calcification of marine plankton in response to increased atmospheric CO_2. *Nature.* **407**(6802), 364–367 (2000).
26. Barker, S. Foraminiferal calcification response to glacial-interglacial changes in atmospheric CO_2. *Science.* **297**(5582), 833–836 (2002).
27. Lombard, F., Da Rocha, R. E., Bijma, J. & Gattuso, J. P. Effect of carbonate ion concentration and irradiance on calcification in planktonic foraminifera. *Biogeosciences.* **7**(1), 247–255 (2010).
28. Iglesias-Rodriguez, M. D. *et al*. Phytoplankton calcification in a high-CO_2 world. *Science.* **320**(5874), 336–340 (2008).
29. Keir, R. S. Dissolution kinetics of biogenic calcium carbonates in seawater. *Geochim Cosmochim Ac.* **44**(2), 241–252 (1980).
30. Hales, B. & Steve, E. Evidence in support of first-order dissolution kinetics of calcite in seawater. *Earth Planet Sc Lett.* **148**(1), 317–327 (1997).
31. Jahnke, R. A., Craven, D. B. & Gaillard, J. F. The influence of organic-matter diagenesis on $CaCO_3$ dissolution at the deep-sea floor. *Geochim Cosmochim Ac.* **58**(13), 2799–2809 (1994).
32. Martin, W. R. & Sayles, F. L. $CaCO_3$ dissolution in sediments of the Ceara Rise, western equatorial. *atlantic. Geochim cosmochim Ac.* **60**(2), 243–263 (1996).
33. Subhas, A. V. *et al*. A novel determination of calcite dissolution kinetics in seawater. *Geochim Cosmochim Ac.* **170**, 51–68 (2015).
34. Subhas, A. V. *et al*. Catalysis and chemical mechanisms of calcite dissolution in seawater. *P Natl Acad Sci USA.* **114**(31), 8175–8180 (2017).
35. Jin, S. *et al*. Decline in the species richness contribution of Echinodermata to the macrobenthos in the shelf seas of China. *Phys Chem Earth.* **87–88**, 43–49 (2015).
36. Liu, W. & He, M. Effects of ocean acidification on the metabolic rates of three species of bivalve from southern coast of China. *Chin J Oceanol Limn.* **30**(2), 206–211 (2012).
37. FAO. The state of world fisheries and aquaculture 2018 - Meeting the sustainable development goals (Food and Agriculture Organization of the United Nations, Rome, 2018).
38. Orr, J. C. *et al*. Anthropogenic ocean acidification over the twenty-first century and its impact on calcifying organisms. *Nature.* **437**(7059), 681–686 (2005).
39. McNeil, B. I. & Matear, R. J. Climate change feedbacks on future oceanic acidification. *Tellus B.* **59**(2), 191–198 (2007).
40. Caldeira, K. & Wickett, M. E. Ocean model predictions of chemistry changes from carbon dioxide emissions to the atmosphere and ocean. *Journal of Geophysical Research.* **110**(C9), C09S04 (2005).
41. Zhai, W. Exploring seasonal acidification in the Yellow Sea. *Sci China Earth Sci.* **61**(6), 647–658 (2018).
42. Xu, X. *et al*. Aragonite saturation state variation and control in the river-dominated marginal BoHai and Yellow seas of China during summer. *Mar Pollut Bull.* **135**, 540–550 (2018).
43. Chou, W. C., Gong, G. C., Hung, C. C. & Wu, Y. H. Carbonate mineral saturation states in the East China Sea: present conditions and future scenarios. *Biogeosciences.* **10**(10), 6453–6467 (2013).
44. Xu, X., Wu, J. & Liu, P. Research progress of ocean acidification and its ecological efficiency in China. *Fisheries Sci.* **35**(6), 735–740 (2016).
45. Weaver, A. J. *et al*. The UVic Earth System Climate Model: Model description, climatology, and applications to past, present and future climates. *Atmos ocean.* **39**(4), 361–428 (2001).
46. Schmittner, A., Oschlies, A., Matthews, H. D. & Galbraith, E. D. Future changes in climate, ocean circulation, ecosystems, and biogeochemical cycling simulated for a business-as-usual CO_2 emission scenario until year 4000 AD. *Global Biogeochem Cy.* **22**(1), GB1013 (2008).
47. Schmittner, A., Oschlies, A., Giraud, X., Eby, M. & Simmons, H. L. A global model of the marine ecosystem for long-term simulations: Sensitivity to ocean mixing, buoyancy forcing, particle sinking, and dissolved organic matter cycling. *Global Biogeochem Cy.* **19**(3), B3004 (2005).
48. Cao, L., Wang, S., Zheng, M. & Zhang, H. Sensitivity of ocean acidification and oxygen to the uncertainty in climate change. *Environ Res Lett.* **9**(6), 064005 (2014).
49. Cao, L. *et al*. The role of ocean transport in the uptake of anthropogenic CO_2. *Biogeosciences.* **6**(3), 375–390 (2009).
50. Key, R. M. *et al*. A global ocean carbon climatology: Results from Global Data Analysis Project (GLODAP). *Global biogeochem cy.* **18**(4), GB4031 (2004).
51. Gazeau, F. *et al*. Impact of elevated CO_2 on shellfish calcification. *Geophys Res Lett.* **34**(7), L7603 (2007).

52. Bernardello, R. *et al*. Response of the ocean natural carbon storage to projected twenty-first-century climate change. *J Climate.* **27**(5), 2033–2053 (2014).
53. Schwinger, J. *et al*. Nonlinearity of ocean carbon cycle feedbacks in CMIP5 Earth system models. *J Climate.* **27**(11), 3869–3888 (2014).
54. Wu, Y. & Gao, K. Combined effects of solar UV radiation and CO_2-induced seawater acidification on photosynthetic carbon fixation of phytoplankton assemblages in the South China Sea. *Chinese Sci Bull.* **55**(32), 3680–3686 (2010).
55. Ishimatsu, A. & Dissanayake, A. Life threatened in acidic coastal waters in *Coastal Environmental and Ecosystem Issues of the East China Sea* (ed. Ishimatsu, A. & Lie, H.) 283–303 (TERRAPUB and Nagasaki University, Tokyo, 2010).
56. Doney, S. C., Fabry, V. J., Feely, R. A. & Kleypas, J. A. Ocean acidification: The other CO_2 problem. *Annu Rev Mar Sci.* **1**, 169–192 (2009).
57. Wang, K., Ma, H., Li, J., Gu, B. & Wu, H. Assessment of the POEM2 model for simulating tropical intraseasonal oscillation. *J Trop Meteorol.* **24**(3), 323–333 (2018).
58. Ridgwell, A. & Hargreaves, J. C. Regulation of atmospheric CO_2 by deep-sea sediments in an Earth system model. *Global Biogeochem Cy.* **21**(2), GB2008 (2007).
59. Archer, D. Fate of fossil fuel CO_2 in geologic time. *J Geophys Res-Oceans.* **110**(C9), C09S05 (2005).
60. Broecker, W. & Peng, T. The role of $CaCO_3$ compensation the glacial to interglacial atmospheric CO_2 change. *Global Biogeochem Cy.* **1**(1), 15–29 (1987).
61. Fanning, A. F. & Weaver, A. J. An atmospheric energy-moisture balance model: Climatology, interpentadal climate change, and coupling to an ocean general circulation model. *J Geophys Res-Atmos.* **101**(D10), 15111–15128 (1996).
62. Pacanowski, R. MOM 2 documentation user's guide and reference manual in *GFDL Ocean Group Technical Report 3.2* (NOAA, GFDL, Princeton, 1995).
63. Hunke, E. C. & Dukowicz, J. K. An elastic-viscous-plastic model for sea ice dynamics. *J Phys Oceanogr.* **27**(9), 1849–1867 (1997).
64. Bitz, C. M., Holland, M. M., Weaver, A. J. & Eby, M. Simulating the ice-thickness distribution in a coupled climate model. *J Geophys Res-Oceans.* **106**(C2), 2441–2463 (2001).
65. Cox, P. M. Description of the "TRIFFID" dynamic global vegetation model (Hadley Centre, Met Office, 2001).
66. Meissner, K. J., Weaver, A. J., Matthews, H. D. & Cox, P. M. The role of land surface dynamics in glacial inception: a study with the UVic Earth System Model. *Clim Dynam.* **21**(7–8), 515–537 (2003).
67. Schmittner, A., Oschlies, A., Damon Matthews, H. & Galbraith, E. D. Correction to "Future changes in climate, ocean circulation, ecosystems, and biogeochemical cycling simulated for a business-as-usual CO_2 emission scenario until year 4000 AD". *Global Biogeochem Cy.* **23**(3), GB3005 (2009).
68. Orr, J. C., Najjar, R., Sabine, C. L. & Joos, F. Design of OCMIP-2 simulations of chlorofluorocarbons, the solubility pump and common biogeochemistry (LSCE/CEA, 1999).
69. Eby, M. *et al*. Historical and idealized climate model experiments: an intercomparison of Earth system models of intermediate complexity. *Clim Past.* **9**(3), 1111–1140 (2013).
70. Zickfeld, K. *et al*. Long-term climate change commitment and reversibility: An EMIC intercomparison. *J Climate.* **26**(16), 5782–5809 (2013).
71. Friedlingstein, P. *et al*. Climate-carbon cycle feedback analysis, results from the C^4MIP model intercomparison. *J Climate.* **19**(14), 3337–3353 (2006).
72. Weber, S. L. *et al*. The modern and glacial overturning circulation in the Atlantic Ocean in PMIP coupled model simulations. *Clim Past.* **3**(1), 51–64 (2007).
73. Gregory, J. M. *et al*. A model intercomparison of changes in the Atlantic thermohaline circulation in response to increasing atmospheric CO_2 concentration. *Geophys Res Lett.* **32**(12), L12703 (2005).
74. Stouffer, R. J. *et al*. Investigating the causes of the response of the thermohaline circulation to past and future climate changes. *J Climate.* **19**(8), 1365–1387 (2006).
75. Turley, C. *et al*. The societal challenge of ocean acidification. *Mar Pollut Bull.* **60**(6), 787–792 (2010).
76. Matthews, H. D., Cao, L. & Caldeira, K. Sensitivity of ocean acidification to geoengineered climate stabilization. *Geophys Res Lett.* **36**, L10706 (2009).
77. Alexander, K., Meissner, K. J. & Bralower, T. J. Sudden spreading of corrosive bottom water during the Palaeocene-Eocene Thermal Maximum. *Nat Geosci.* **8**(6), 457–458 (2015).
78. Bralower, T. J., Meissner, K. J., Alexander, K. & Thomas, D. J. The dynamics of global change at the Paleocene-Eocene thermal maximum: A data-model comparison. *Geochem Geophy Geosy.* **15**(10), 3830–3848 (2014).
79. Xiao, D., Zhou, X. & Zhao, P. Numerical simulation study of temperature change over East China in the past millennium. *Sci China Earth Sci.* **55**(9), 1504–1517 (2012).
80. Meissner, K. J. Younger Dryas: A data to model comparison to constrain the strength of the overturning circulation. *Geophys Res Lett.* **34**(21), L21705 (2007).
81. Weaver, A. J., Eby, M., Kienast, M. & Saenko, O. A. Response of the Atlantic meridional overturning circulation to increasing atmospheric CO_2: Sensitivity to mean climate state. *Geophys Res Lett.* **34**(5), L05708 (2007).
82. Spence, J. P. & Weaver, A. J. The impact of tropical Atlantic freshwater fluxes on the North Atlantic meridional overturning circulation. *J climate.* **19**(18), 4592–4604 (2006).
83. Muglia, J. & Schmittner, A. Glacial Atlantic overturning increased by wind stress in climate models. *Geophys Res Lett.* **42**(22), 9862–9869 (2015).
84. Meinshausen, M. *et al*. The RCP greenhouse gas concentrations and their extensions from 1765 to 2300. *Climatic change.* **109**(1-2), 213–241 (2011).
85. Huang, J., Yu, H., Dai, A., Wei, Y. & Kang, L. Drylands face potential threat under 2 degrees C global warming target. *Nat Clim Change.* **7**(6), 417 (2017).
86. Zeebe, R. E. & Wolf-Gladrow, D. A., *CO_2 in seawater: equilibrium*, *kinetics*, *isotopes*. (Gulf Professional Publishing, 2001).
87. Zeebe, R. E. History of seawater carbonate chemistry, atmospheric CO_2, and ocean acidification in *Annual Review of Earth and Planetary Sciences* (ed. Jeanloz, R.) 141–165, Vol. 40 (2012).

Acknowledgements

This study is supported by the National Key R&D Program of China (2017YFC1502303), the Natural Science Foundation of Zhejiang Province (LQ20D050003), the Natural Science Foundation of China (41605049), the Fund for Meteorological Science and Technology of Zhejiang Province (2019YB03), and Special Program on Climate Change of China Meteorological Administration (CCSF201916-1).

Author contributions

H.Z. and K.W. designed the research. H.Z. and K.W. performed model simulations and analysis. Both H.Z. and K.W. contributed to the writing of the paper.

Competing interests
The authors declare no competing interests.

Additional information
Supplementary information is available for this paper at https://doi.org/10.1038/s41598-019-54861-0.

Correspondence and requests for materials should be addressed to K.W.

Reprints and permissions information is available at www.nature.com/reprints.

Publisher's note Springer Nature remains neutral with regard to jurisdictional claims in published maps and institutional affiliations.